Global Precipitation and Thunderstorm Frequencies. Part II: Diurnal Variations

AIGUO DAI

National Center for Atmospheric Research, Boulder, Colorado*

(Manuscript received 24 January 2000, in final form 8 May 2000)

ABSTRACT

Three-hourly present weather reports from ~15 000 stations around the globe and from the Comprehensive Ocean–Atmosphere Data Set from 1975 to 1997 were analyzed for diurnal variations in the frequency of occurrence for various types of precipitation (drizzle, nondrizzle, showery, nonshowery, and snow) and thunderstorms. Significant diurnal variations with amplitudes exceeding 20% of the daily mean are found over much of the globe, especially over land areas and during summer. Drizzle and nonshowery precipitation occur most frequently in the morning around 0600 local solar time (LST) over most land areas and from midnight to 0400 LST over many oceanic areas. Showery precipitation and thunderstorms occur much more frequently in the late afternoon than other times over most land areas in all seasons, with a diurnal amplitude exceeding 50% of the daily mean frequencies. Over the North Pacific, the North Atlantic, and many other oceanic areas adjacent to continents, showery precipitation is most frequent in the morning around 0600 LST, which is out of phase with land areas. Over the tropical and southern oceans, showery precipitation tends to peak from midnight to 0400 LST. Maritime thunderstorms occur most frequently around midnight. It is suggested that the diurnal variations in atmospheric relative humidity contribute to the morning maximum in the frequency of occurrence for drizzle and nonshowery precipitation, especially over land areas. Solar heating on the ground produces a late-afternoon maximum of convective available potential energy in the atmosphere that favors late-afternoon moist convection and showery precipitation over land areas during summer. This strong continental diurnal cycle induces a diurnal cycle of opposite phase in low-level convergence over large nearby oceanic areas that favors a morning maximum of maritime showery precipitation. Larger low-level convergence induced by pressure tides and higher relative humidity at night than at other times may contribute to the nighttime maximum of maritime showery and nonshowery precipitation over remote oceans far away from continents.

1. Introduction

Documentation of the diurnal variability of precipitation over various regions has been a topic of hundreds of published articles. Studies before 1975 have been summarized by Wallace (1975). Dai et al. (1999a) summarized more recent analyses for the United States (e.g., Schwartz and Bosart 1979; Balling 1985; Easterling and Robinson 1985; Englehart and Douglas 1985; Riley et al. 1987; Landin and Bosart 1989; Tucker 1993; Higgins et al. 1996). There are also more recent studies for the coastal and island regions in eastern Asia (Hu and Hong 1989; Oki and Musiake 1994; Lim and Kwon 1998), tropical America (Kousky 1980), East Africa (Majugu 1986), and the Sahel (Shinoda et al. 1999). The results of these studies, which are based on station records, can be summarized as follows: 1) summer precipitation and thunderstorms over inland regions tend to be more frequent during the afternoons while the maximum rainfall is at night or during early morning over the coastal and small-island areas. 2) There are, however, exceptions to this general tendency. For example, summer precipitation is most frequent from middle night to early morning over the central United States and around 1400–1600 local solar time (LST) over the entire Florida Peninsula (Wallace 1975; Dai et al. 1999a). 3) During the other seasons, precipitation has a much weaker diurnal cycle than in summer, with a morning maximum in winter over many land areas (Dai et al. 1999a). 4) Precipitation intensity generally has much smaller diurnal variations than precipitation frequency (Oki and Musiake 1994; Dai et al. 1999a). 5) Although a single large peak is a dominant feature in most station rain gauge records, there is a secondary peak or a weak semidiurnal (12-h) cycle of rainfall at many tropical (peak around 0300 LST) and midlatitude (peak around 0600 LST) stations (Hamilton 1981a,b; Oki and Musiake 1994).

Over the open oceans, in situ observations of precipitation are sparse. Kraus (1963) analyzed weather reports from nine fixed weather-ships in the northern (30°–

* The National Center for Atmospheric Research is sponsored by the National Science Foundation.

Corresponding author address: A. Dai, National Center for Atmospheric Research, P.O. Box 3000, Boulder, CO 80307-3000.
E-mail: adai@ucar.edu

58°N) Atlantic and Pacific and found that maritime precipitation is significantly more frequent at night, with a maximum around 0300 LST. Rain gauge data from small tropical islands in the western and central Pacific also show large early morning maxima (Gray and Jacobson 1977). A widespread nocturnal maximum in oceanic thunderstorm activity is also evident in ship weather reports (Sanders and Freeman 1983). However, afternoon maxima were also found in rainfall records over the Global Atmospheric Research Program (GARP) Atlantic Tropical Experiment (GATE) region (about 5°–10°N and 20°–27°W) over the tropical Atlantic (Gray and Jacobson 1977; McGarry and Reed 1978).

In the Tropics, convective showery precipitation occurs more frequently than nonshowery precipitation and the latter seems to be related to the former (Dai 2001). Diurnal variations of tropical rainfall are therefore closely linked to moist convection. Because of the scarcity of rainfall data over the oceans, various proxies of maritime rainfall and deep convection have been applied to investigate the diurnal variability of precipitation over the low-latitude oceans. For example, Riehl and Miller (1978), Albright et al. (1985), Meisner and Arkin (1987), Shin et al. (1990), Janowiak et al. (1994), and Garreaud and Wallace (1997) employed satellite infrared data; Short and Wallace (1980), Hartmann and Recker (1986), and Gruber and Chen (1988) used outgoing longwave radiation data; Sharma et al. (1991), Negri et al. (1994), and Chang et al. (1995) applied passive microwave data; Fu et al. (1990) examined satellite-derived convective clouds; and Hendon and Woodberry (1993) analyzed indices of deep convection and global cloudiness. Despite the coarse temporal-sampling resolution (2 times per day) in some of the satellite data, most of these studies confirm the existence of a morning maximum in oceanic convection and rainfall, with the amplitude reaching about half or more of the daily mean value. However, afternoon maxima were also found over some oceanic areas such as the tropical eastern Atlantic (Reed and Jaffe 1981), the South Pacific convergence zone (SPCZ; Albright et al. 1985), and the tropical central and eastern Pacific (Augustine 1984). Over the tropical western Pacific, afternoon maxima of convection and rainfall were also found during the periods when there are few large-scale convective systems passing by and the diurnal cycle of sea surface temperature (SST) is strong (Sui et al. 1997). An analysis of global surface wind divergence fields by Dai and Deser (1999) shows that while surface convergence peaks in the morning (around 0600 LST) over many oceanic areas close to continents, afternoon maximum convergence also occurs over many open oceans. This again suggests that the diurnal cycle in oceanic convection and rainfall may have different phases over different regions.

A number of physical mechanisms have been proposed to explain the observed diurnal variations in precipitation and tropical convection. Wallace (1975) suggested that the coastal land and sea-breeze circulation, the solar heating over the sloping terrain, and diurnal changes in frictional drag of the planetary boundary layer may induce diurnal variations in low-level convergence that largely control the timing of convective rainfall over land and coastal areas during summer. Dai et al. (1999a) show that tidal variations in surface pressure fields (Dai and Wang 1999) can induce substantial diurnal variations in low-level convergence with phases consistent with those of summer rainfall across the United States. The diurnal phase patterns of surface wind divergence (Dai and Deser 1999) suggest that there exists a large-scale diurnal circulation in which surface air converges and rises over continents (except for the innermost parts) and diverges and sinks over large nearby oceanic areas in the afternoon and early evening and the opposite occurs in the early morning. This thermally driven land–ocean diurnal circulation may contribute to the general pattern of afternoon rainfall maxima over land areas and early morning rainfall maxima over the adjacent oceans, as suggested by Silva Dias et al. (1987) for South America.

Rainfall diurnal cycles exist, however, even in a general circulation model (GCM) without landmasses, although the amplitude was reduced (Randall et al. 1991). This suggests that there exist other mechanisms for the rainfall diurnal cycle over the oceans far away from land areas. Malkus (1964) and Brier and Simpson (1969) suggested and Dai et al. (1999a) showed (over the United States) that the diurnal timing of rainfall is strongly influenced by the pressure tides [which can induce a diurnal amplitude of $\sim 10^{-6}$ s^{-1} in low-level convergence resulting from the spatial gradients in the phase and amplitude of the tides (Dai et al. 1999a)], although the importance of this mechanism was questioned by Lindzen (1978). Gray and colleagues (Gray and Jacobsen 1977; Foltz and Gray 1979) have suggested that the diurnal timing of oceanic precipitation results from a diurnal cycle of low-level divergence that should be maximum over relatively clear-sky areas and minimum over cloudy regions at the end of the night due to the fact that atmospheric radiative cooling at night is larger over clear-sky than cloudy areas. The diurnal phase pattern of surface wind divergence over the central Pacific from 10°–25°N to 25°–45°N and over the equatorial intertropical convergence zone (ITCZ) regions is correlated with cloudiness over these regions in a manner that seems to broadly support Gray's radiative cooling hypothesis (but not over the South Pacific) (Dai and Deser 1999). Other proposed mechanisms include cloud-radiation interactions (absorption of solar radiation at cloud tops stabilizes the clouds during the day while longwave cooling of the cloud tops destabilizes the environment and promotes convection) (e.g., Kraus 1963; Randall et al. 1991; Xu and Randall 1995), daytime heating of the sea surface (Hendon and Woodberry 1993; Chen and Houze 1997), and day–night differences in available precipitable water (Sui et al. 1997). Model experiments suggest that some of these mechanisms may

play complementary roles in the diurnal cycle of oceanic precipitation (Randall et al. 1991). However, the relative importance of these mechanisms is likely to vary over different regions and this needs further investigation.

Previous studies of diurnal variations of precipitation used data from a limited number of stations or a regional domain and focused on total precipitation. Consequently, the large-scale spatial patterns in the amplitude and phase of the diurnal cycle of precipitation and the differences of the diurnal cycle among various types of precipitation (e.g., showery versus nonshowery) have not been studied on a global scale. In this study, we analyze the present weather reports from station and ship observations to derive a near-global (50°S–70°N) climatology of the diurnal cycle of the frequency of occurrence[1] for various types of precipitation (drizzle, nondrizzle, showery, nonshowery, and snow) and thunderstorms. Despite many potential biases in the weather reports, they represent one of a few in situ observations of precipitation characteristics on a global scale (Dai 2001). Our results show a clear picture of the large-scale spatial patterns in the diurnal cycle of various types of precipitation and should provide insights into the relative importance of underlying mechanisms for the diurnal variations over various regions.

2. Data and analysis method

The 3-hourly present[2] (WMO code ''ww'') weather data for the 1975–97 period were extracted from synoptic reports from ~15 000 land, island, and ocean stations included in the Global Telecommunication System (GTS) and from shipboard observations (about 3–5 $\times$ 10^6 reports yr^{-1}) included in the Comprehensive Ocean–Atmosphere Data Set (COADS) (Woodruff et al. 1993). The quality of these data and the procedure to derive the frequency of occurrence for drizzle, nondrizzle precipitation (including all forms of precipitation except drizzles), showery precipitation, nonshowery precipitation, thunderstorms (including nonprecipitating ones), and snow were described in detail by Dai (2001), except that here the frequency for each of the observation times (0000, 0300, 0600 UTC, etc.) was analyzed. Here, we shall only describe the method for analyzing the diurnal variations.

Station and ship weather reports within each 2° lat $\times$ 2° long grid box were counted through the whole data period to derive a mean frequency of occurrence for the grid box.[3] The counting was done by season and for each of the precipitation types. The mean 3-hourly frequency (F) at each grid box was then subjected to a harmonic analysis:

$$F(t') = F_0 + S_1(t') + S_2(t') + \text{residual} \quad \text{and} \quad (1)$$

$$S_n(t') = A_n \sin(nt' + \sigma_n)$$
$$= a_n \cos(nt') + b_n \sin(nt'), \quad (2)$$

where $n = 1, 2$ (for diurnal and semidiurnal cycles), F_0 is the daily mean value, S_1 and S_2 are the diurnal and semidiurnal harmonics, respectively, A_n is the amplitude (note that the peak-to-peak amplitude is $2A_n$), σ_n is the phase, and t' is mean LST expressed in degrees or radians (i.e., $t' = 2\pi t_1/24$, where t_1 is LST in hours). The residual in Eq. (1) contains the higher-order harmonics of the daily variations that are not resolved by the 3-hourly sampling. Since previous analyses of hourly data (e.g., Wallace 1975; Hamilton 1981a,b; Oki and Musiake 1994) showed that these high-frequency harmonics are much smaller than S_1 and S_2, the error induced by the aliasing of the higher-order harmonics is likely to be small in Eqs. (1) and (2).

Examples of the fitted diurnal and semidiurnal cycles of the frequencies for nondrizzle and showery precipitation are shown in Figs. 1 and 2, respectively. It can be seen that while the diurnal harmonic dominates the daily variations at most of the land locations, the semidiurnal harmonic is significant (in comparison with S_1) at the oceanic boxes. Both the nondrizzle and showery precipitation frequencies peak in the afternoon at the land boxes while a morning maximum is evident at the ocean boxes. It should be emphasized that while the diurnal and semidiurnal harmonics can represent the daily variations reasonably well over majority of the locations, they fit the data poorly at some land and ocean boxes, especially when the number of observations is small and/or the daily variations are weak. We shall use the percentage of the mean daily variance explained by the two harmonics as a measure of the goodness of fit. Because the data are insufficient for resolving the semidiurnal harmonic (requiring eight samples per day) over many of the tropical Pacific and southern (south of ~35°S) oceans (Dai 2001), we shall focus on the diurnal harmonic (S_1).

The harmonic coefficients a_n and b_n were then expanded using trigonometric series of the longitude so that the relative importance of various zonal modes with different wave numbers can be examined [see Dai and Wang (1999) for details of this method].

The anomaly data of the June–August (JJA) mean frequency of occurrence for nondrizzle and showery precipitation (expressed as departures from the daily mean)

[1] The frequency of occurrence is defined here as the number of reports of a precipitation type or thunderstorms divided by the number of total weather reports. It may be expressed in a fraction or percentage and also referred to as precipitation frequency for short.

[2] At the time of observation or during the preceding hour.

[3] Tests showed that computing amplitudes and phases at each station and then averaging them within each grid box yielded similar results.

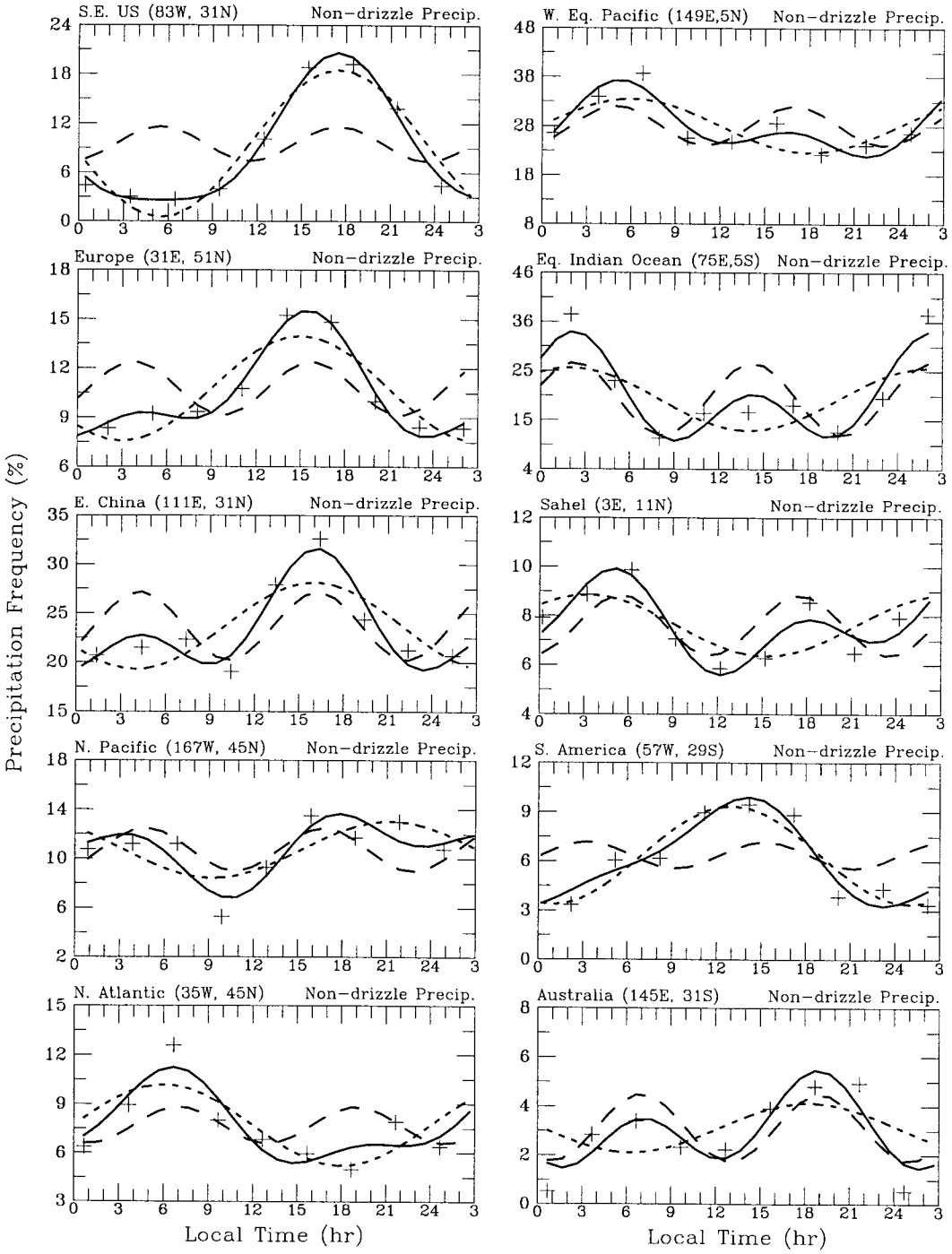

FIG. 1. Observed 1975–97 mean frequency of occurrence for nondrizzle precipitation (pluses) together with the fitted diurnal (short-dashed curve) and semidiurnal (long-dashed curve) harmonics at 10 locations. The solid curve is the sum of the two harmonics. The data are for Jun–Aug except for South America and Australia where they are for Dec–Feb.

are shown in Fig. 3 for the 6-hourly observation times. Figure 3 shows that while the westward propagating wavenumber 1 and 2 modes appear to exist in the anomaly data, the dominant modes are not as clear as in surface pressure (Dai and Wang 1999) and surface wind fields (Dai and Deser 1999). The land and ocean areas appear to be out of phase (e.g., over Eurasia and the Indian Ocean). The dominant wave modes will become more clear in the zonal harmonic analysis of the data, while the phase patterns will appear in the harmonic analysis.

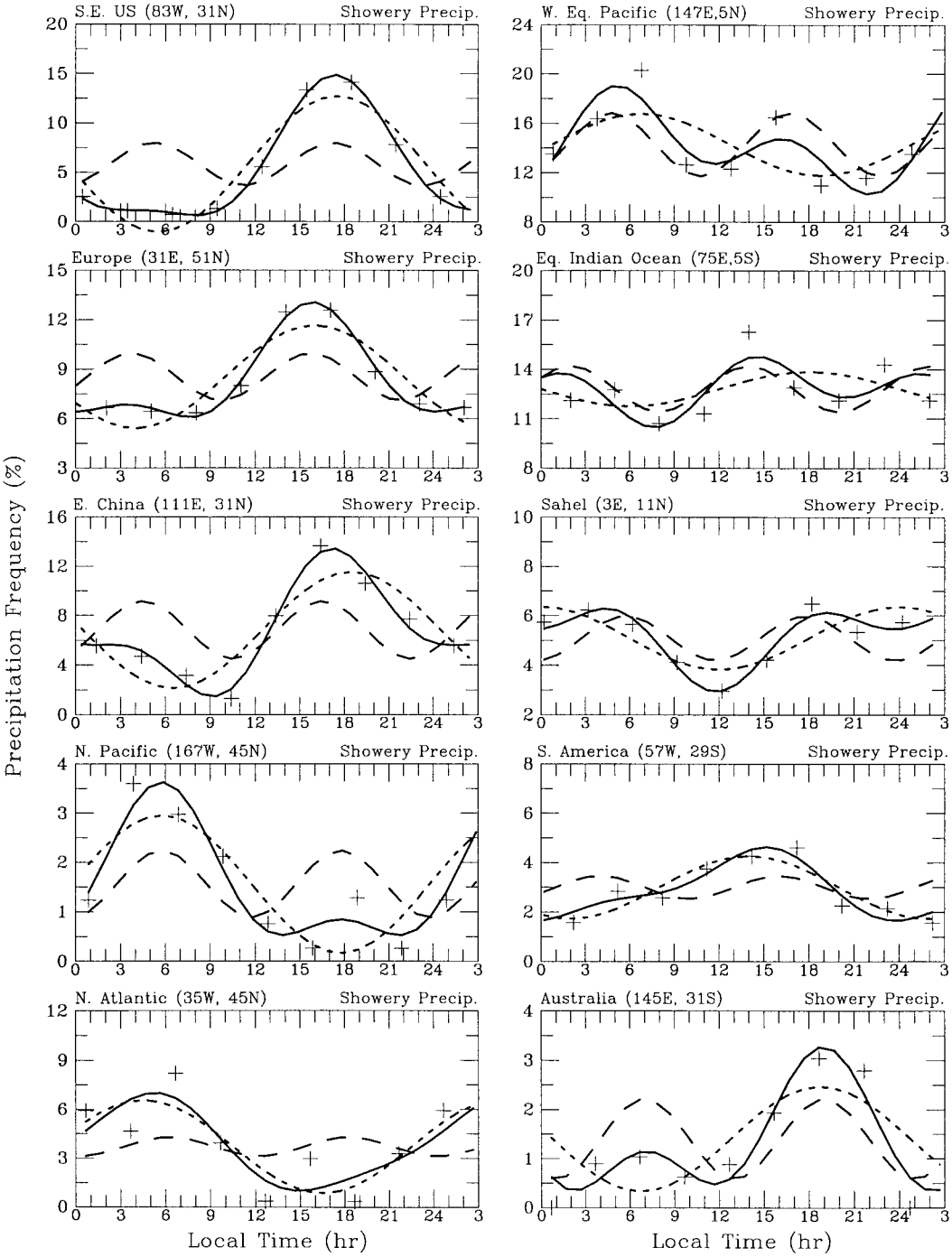

FIG. 2. Same as Fig. 1 but for showery precipitation.

3. Results

a. The significance of the diurnal (S_1) and semidiurnal (S_2) cycles

Before describing the phase and amplitude of the diurnal and semidiurnal cycles, we should know how significant these two harmonics are. To answer this question, we need to know how large the diurnal variations are and how well the two harmonics represent them. As shown by Figs. 1 and 2 (and later by the amplitude maps) and by earlier studies cited in the introduction, the diurnal variations in the frequency of occurrence for the precipitation types and thunderstorms are significant compared with the daily mean at least during summer.

One convenient measure for the representativeness for the diurnal variations is the percentage of the total

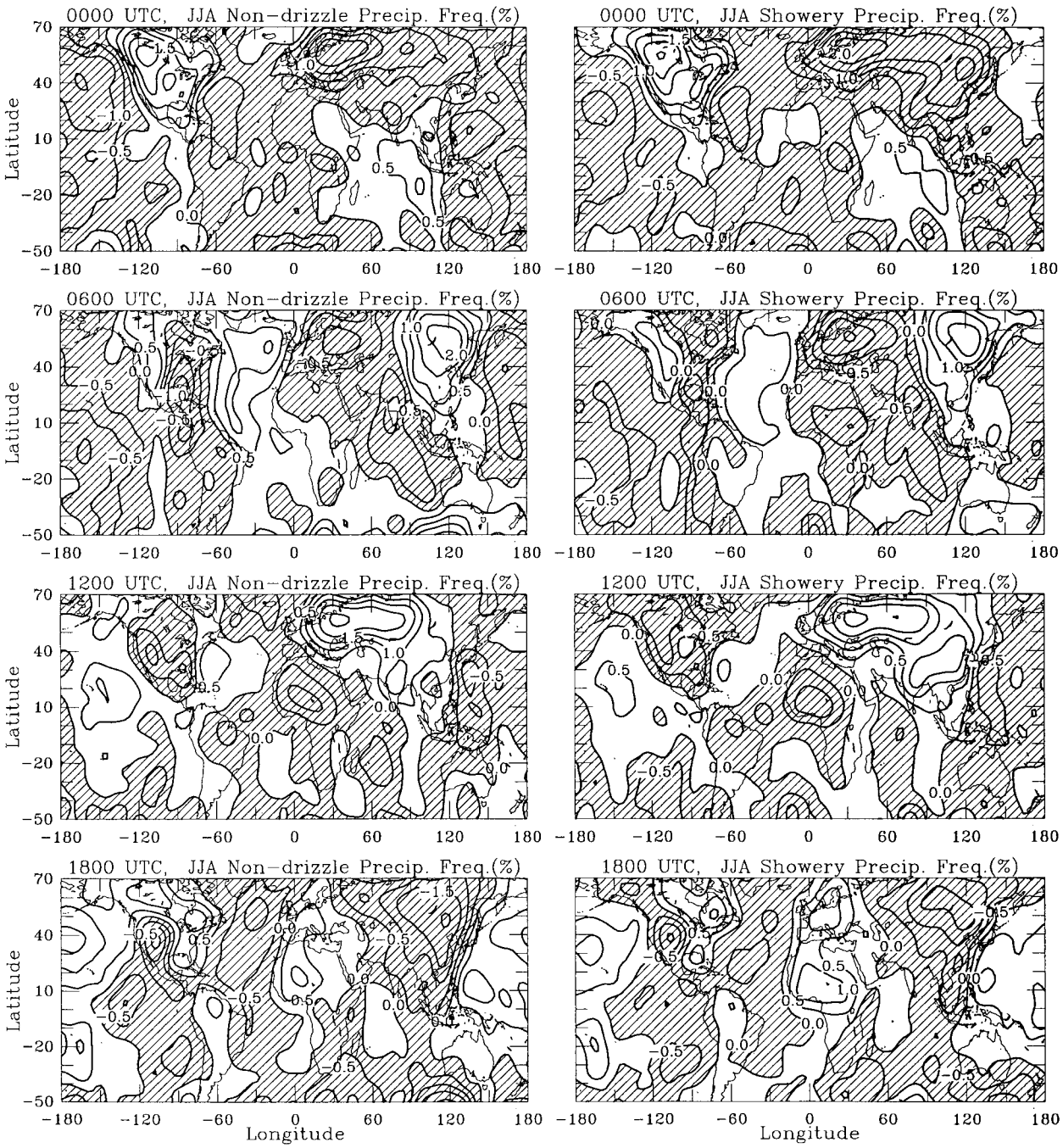

FIG. 3. Mean JJA frequency of occurrence for (left) nondrizzle and (right) showery precipitation (expressed as departures from the daily mean) at the 6-hourly observation times derived from station and shipboard weather reports of the 1975–97 period. Negative values are hatched. Contour intervals are 0.5%.

daily variance[4] explained by the two harmonics. Figure 4 shows that during JJA (and the other seasons, not shown) the diurnal cycle (S_1) accounts for about 40% of the mean daily variance over the oceans for all the precipitation types and thunderstorms. Over land areas, the S_1 explains considerably higher percentages (up to 80%) of the daily variance than over the oceans. In particular, the S_1 accounts for about 60%–80% of the daily variance over Eurasia and North America for showery precipitation and thunderstorms during summer (about 40%–60% in the other seasons). Over eastern Asia and western Europe, the S_1 explains 60%–70%

[4] The total daily variance is defined here as the variance of the mean 3-hourly data such as the 8 data points shown in Figs. 1 and 2.

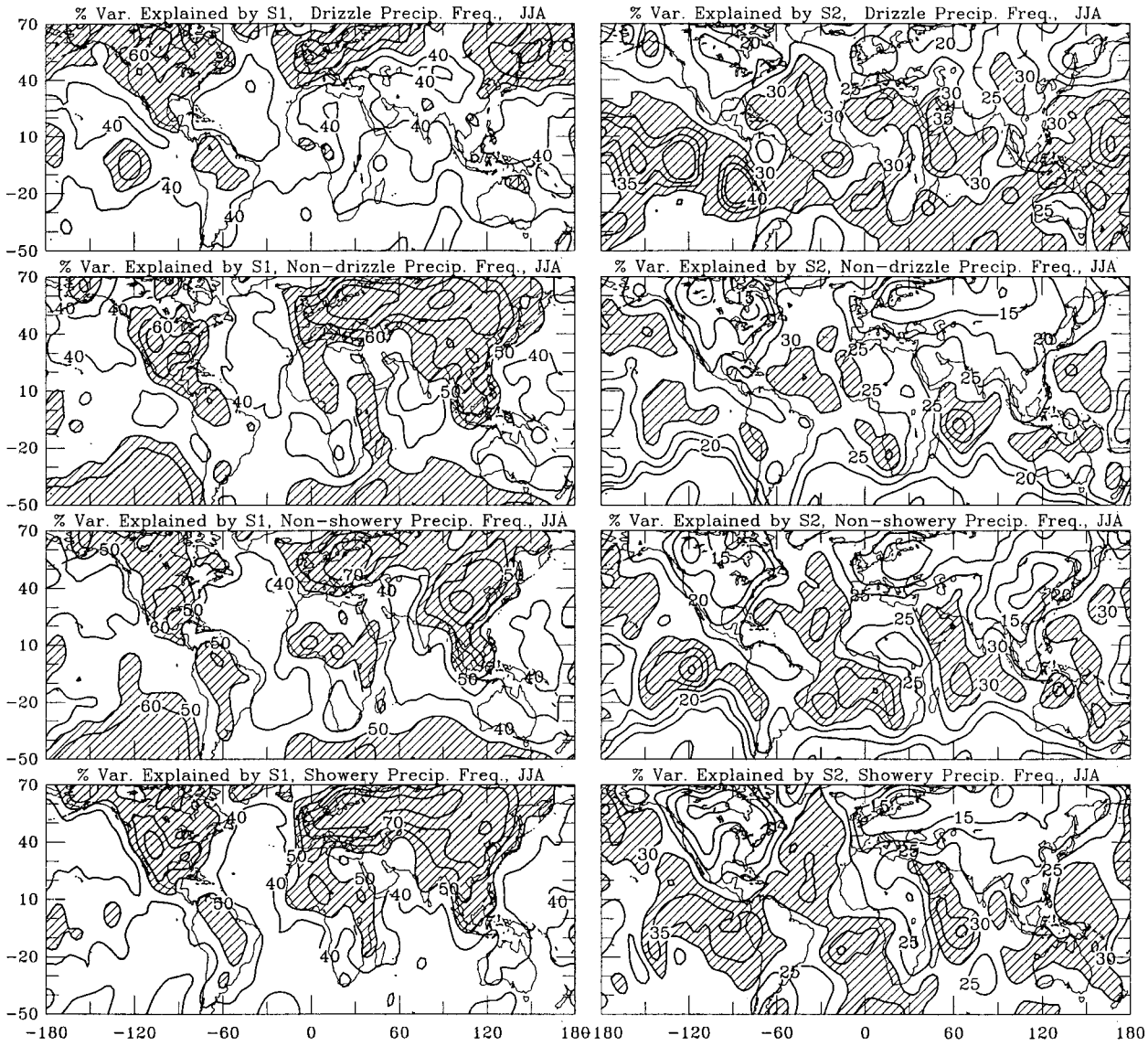

FIG. 4. Percentage of the mean daily variance explained by the (left) diurnal and (right) semidiurnal harmonics for JJA mean frequency of occurrence for (top row) drizzle, (2d row) nondrizzle, (3d row) nonshowery, and (bottom row) showery precipitation. Plots for thunderstorms and winter snow are similar to those for showery precipitation and nonshowery precipitation, respectively. Values over 50% and 30% are hatched in the left and right columns, respectively.

of the daily variance for nonshowery precipitation in JJA (slightly lower in the other seasons). On the other hand, the semidiurnal cycle (S_2) accounts for only ~15%–25% (20%–40%) of the daily variance over land (ocean) areas (Fig. 4). Therefore, the S_1 predominates over land areas whereas the S_1 and S_2 are comparable over the oceans. Together, the S_1 and S_2 explain about 60%–95% of the total daily variance over most of the globe for all the precipitation and thunderstorm frequencies.

The explained percentages of variance by the S_1 and S_2 for the precipitation frequencies are comparable to those for surface winds and surface wind divergence (Dai and Deser 1999). However, the relative strength of the S_2 (compared with the S_1) is considerably weaker than that in surface pressure fields (Dai and Wang 1999).

b. The phase of the diurnal cycle

Figure 5 shows the local solar time when the diurnal harmonic peaks (T_{max}, in hours) for December–February (DJF) and JJA mean frequency of occurrence for drizzle, nondrizzle, nonshowery and showery precipitation, and thunderstorms. It can be seen that for drizzle and nonshowery precipitation, the S_1 tends to peak in the morning around 0600 LST over most land areas and from middle night to 0400 LST over many oceanic areas, although there are regional differences (e.g., the T_{max}

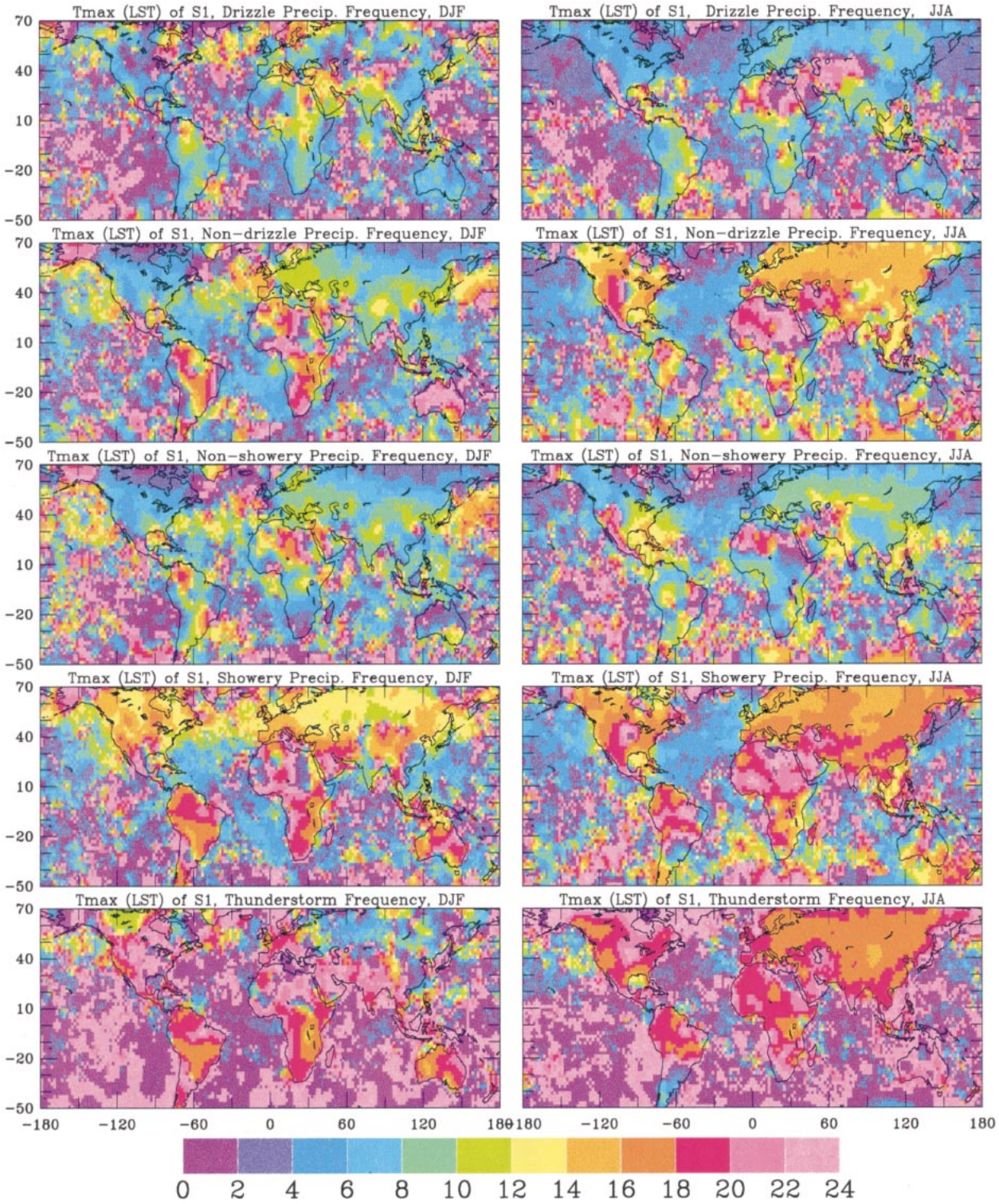

FIG. 5. Local solar time T_{max} (h) when the diurnal harmonic (S_1) of (left) DJF and (right) JJA mean frequency of occurrence peaks for (top row) drizzle, (2d row) nondrizzle, (middle row) nonshowery and (4th row) showery precipitation, and (bottom row) thunderstorms. The broad phase patterns for spring and autumn are similar to those for JJA.

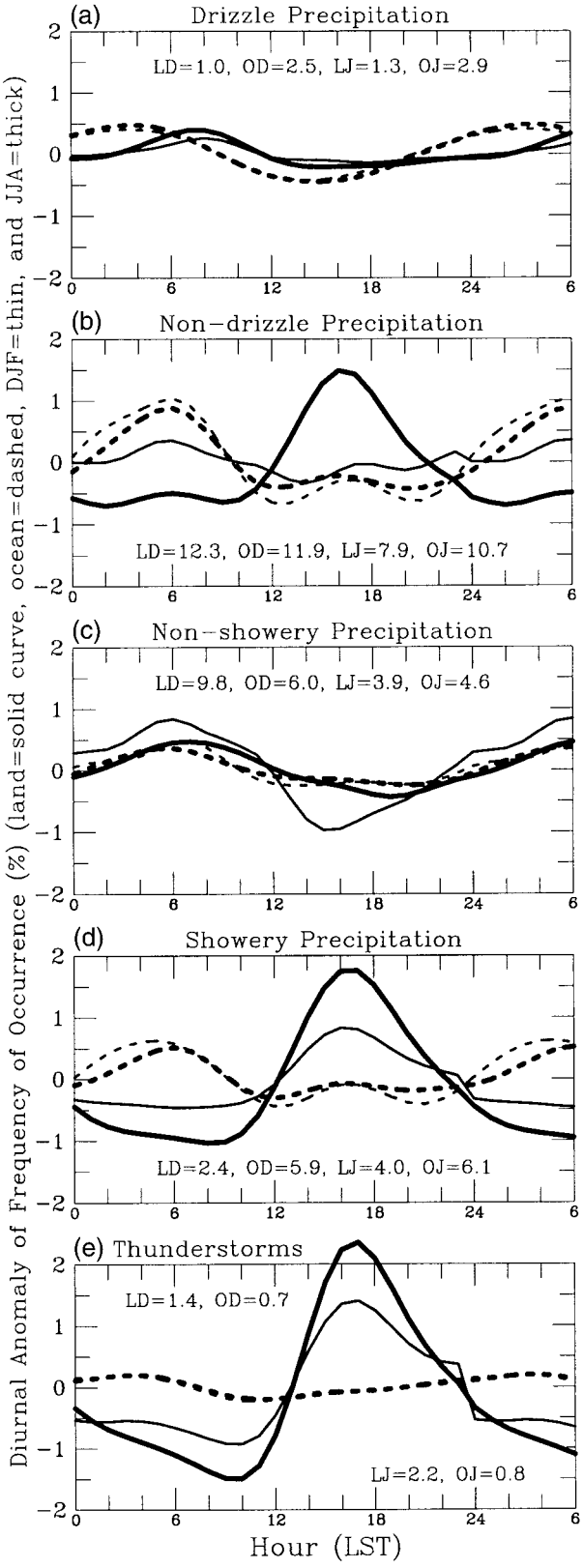

FIG. 6. Observed mean diurnal evolution of the frequency of occurrence (relative to the daily mean) for five precipitation/thunderstorm events area-averaged over the land (solid curves) and ocean (dashed curves) areas within 50°S–70°N for DJF (thin curves) and JJA (thick curves). The averaging was done at each local solar time. Also shown are the daily mean values for DJF land (LD), DJF ocean (OD), JJA land (LJ), and JJA ocean (OJ) areas.

for nonshowery precipitation is around 0600–0800 LST over the North Atlantic south of ~45°N and the tropical western Pacific). Afternoon maxima were also seen for drizzle and nonshowery precipitation frequencies over some regions (e.g., the western North Pacific for DJF nonshowery precipitation).

The morning maximum and afternoon minimum in drizzle and nonshowery precipitation frequencies (Fig. 6) are approximately in phase with the diurnal cycle of relative humidity but out of phase with air temperature in the lower troposphere (Fig. 7). The land–ocean differences of amplitude for the precipitation frequencies (Fig. 6) are also consistent with those for the relative humidity and air temperature. Figure 7 shows that the morning maximum and afternoon minimum in lower tropospheric relative humidity are caused primarily by the diurnal variation of air temperature [which is modulated primarily by clouds and secondly by soil moisture and precipitation (Dai et al. 1999b)], while the specific humidity varies little from day to night. With similar atmospheric contents of water vapor, stratiform precipitation (such as drizzles and nonshowery precipitation) should occur most frequently in the morning as atmospheric relative humidity peaks. Therefore, the morning maxima (and afternoon minima) in the frequency of occurrence for drizzle and nonshowery precipitation over land are caused primarily by the longwave radiative cooling at night and solar heating during the day that are responsible for the diurnal cycle of air temperature. Over the oceans, this mechanism should play a smaller role than over land because of the small diurnal variations in maritime relative humidity (Fig. 7), whereas other mechanisms such as stratiform precipitation from anvil clouds become more important (see below).

For showery precipitation and thunderstorm frequencies, a strong late-afternoon (1500–1900 LST) maximum is evident over most land areas in both summer and winter (and spring and autumn, not shown) (Figs. 5 and 6). Over northern mid- and high-latitude land areas during winter, thunderstorms are rare while showery precipitation is infrequent and often in solid phase (Dai 2001), in contrast to summer showery rainfall, which results from moist convection. Over the central United States, northern Africa and the Middle East, summer showery precipitation and thunderstorms tend to occur most frequently from evening to around midnight (2000–0200 LST). It has been suggested that the eastward propagation of thunderstorms originated over the Rocky Mountains and enhanced nighttime low-level convergence (e.g., resulting from pressure tides) con-

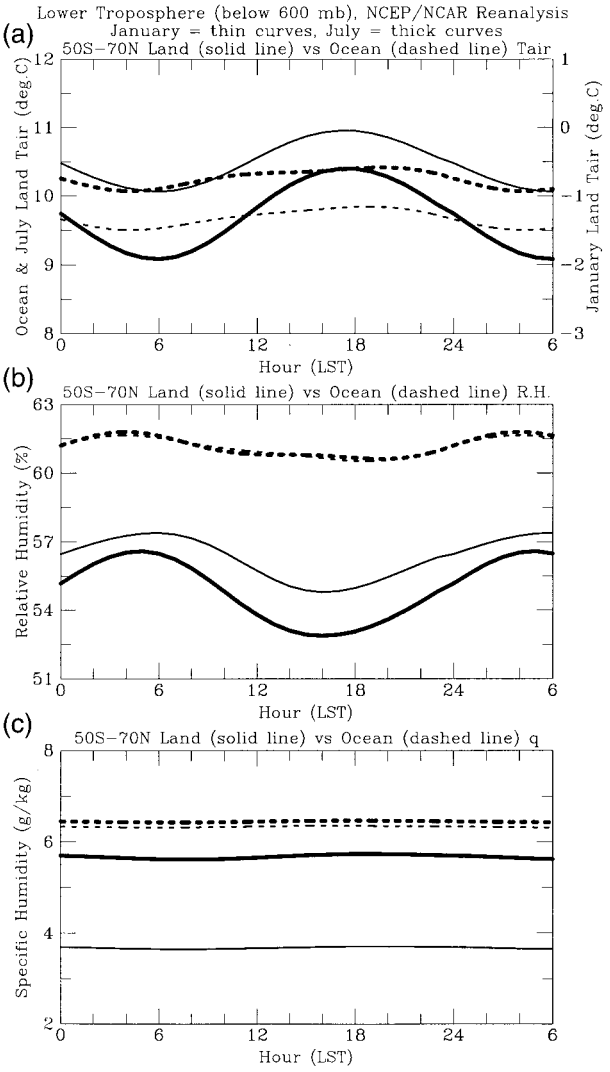

FIG. 7. Mean diurnal evolution of Jan (thin curves) and Jul (thick curves) lower-tropospheric (below 600 mb) (a) mean air temperature, (b) relative humidity, and (c) specific humidity. Note that the Jan land temperature (thin solid curve) is shown on the right ordinate in the top panel, and the curves for Jan and Jul oceanic relative humidity overlap each other. The 6-hourly NCEP–NCAR reanalysis data for 1979–95 (Kalnay et al. 1996) were used in the averaging that was done at each local solar time. Similar diurnal patterns (with larger amplitudes) are also seen in 3-hourly surface observations.

tribute to the nocturnal maximum over the central United States (Dai et al. 1999a).

Over the North Pacific, the North Atlantic (south of ~45° in DJF), and many other oceanic areas adjacent to continents, showery precipitation occurs most frequently in the morning around 0600 LST, which is approximately out of phase with land areas (Fig. 5). Over most of the tropical and southern oceans, where land influences are smaller than over the Northern Hemisphere, showery precipitation peaks from around midnight to 0400 LST, which is about 2–4 h earlier than over the North Pacific and the North Atlantic. Although maritime thunderstorms are infrequent (observed in < 10% of the days; Dai 2001), they occur most frequently around midnight over most of the oceans, except the North Pacific and a few other oceanic regions adjacent to continents where thunderstorms peak around 0400–0600 LST (Fig. 5).

The strong late-afternoon maximum for showery precipitation and thunderstorms over land areas is consistent with the late-afternoon maximum of the convective available potential energy (CAPE)[5] (Fig. 8), a measure of the atmospheric energy available for moist convection. Over land solar heating (primarily through the land surface) during the day produces peak lower-tropospheric temperature (Fig. 7) and CAPE in the late afternoon, which contribute to the late-afternoon maximum frequencies for showery precipitation and thunderstorms over land.

Over the oceans, the CAPE has small diurnal variations (Fig. 8) and is not a driving force for the diurnal cycle of maritime moist convection. During the summer afternoon and evening when the air over continents is warmer than over the nearby oceans, divergence and subsidence should occur over the oceans as air mass converges and rises over continents (as a result of mass conservation). From midnight to early morning, the air over the oceans becomes warmer than over continents (as the land surface cools faster than the ocean surface after the sunset) and the land–ocean circulation reverses. This land–ocean diurnal circulation (superposed on top of the daily mean circulation) is shown in the surface wind divergence fields (Fig. 9) derived from observed 3-hourly surface winds (Dai and Deser 1999). The land–ocean circulation is also evident in the lower-tropospheric pressure velocity (ω) from the National Centers for Environmental Prediction–National Center for Atmospheric Research (NCEP–NCAR) reanalysis (not shown). Therefore, over most of the Northern Hemisphere oceans and many tropical and southern oceans adjacent to continents, the early morning maximum in showery precipitation results primarily from the diurnal cycle of the large-scale land–ocean circulation.

Over the remote tropical and southern oceans, where land influences are relatively small, the midnight to early maximum in showery precipitation and thunderstorms may result from other mechanisms as mentioned in the introduction. For example, Fig. 9 shows a pronounced semidiurnal cycle in surface wind divergence over the tropical and southern oceans. Since semidiurnal pressure tides predominate over these regions (Dai and Wang 1999), it is tempting to hypothesize that atmospheric

[5] Defined as CAPE $= R_d \int_z (T_{vp} - T_{va})\, d\ln p(z)$, where R_d (=287.05 J kg^{-1} K^{-1}) is the gas constant for dry air, T_{vp} and T_{va} are virtual temperatures of an air parcel and the environment, respectively, $p(z)$ is the pressure at height z, and the integration is from the surface up to about 200 mb using the NCEP–NCAR reanalysis data (Kalnay et al. 1996).

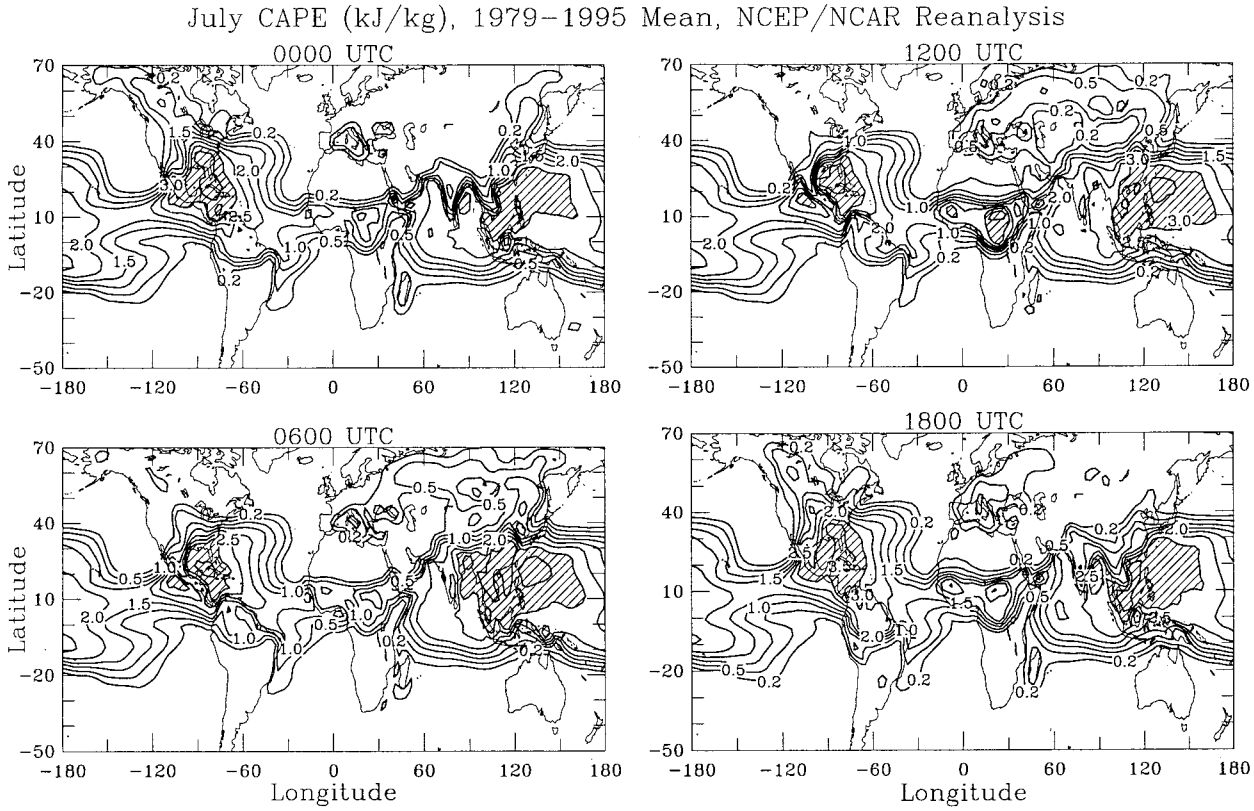

FIG. 8. Mean Jul convective available potential energy (CAPE, kJ kg^{-1}) at 0000, 0600, 1200, and 1800 UTC calculated using the monthly profiles of temperature and humidity from the 6-hourly NCEP–NCAR reanalysis for 1979–95 and then averaged over the period. A pseudo-adiabatic process is used in the calculation.

tidal variations in pressure and wind fields induce early morning convergence (and thus moist convection and showery precipitation) maxima over the open oceans. The semidiurnal tide of surface pressure peaks around 0930–1000 LST (Dai and Wang 1999), which implies maximum convergence around 0300–0400 LST. Considering the large sampling error ($\pm$1.5 h) for the phase shown in Fig. 9, the diurnal phases among surface pressure tides, surface wind divergence, and showery precipitation over the tropical and southern oceans are not inconsistent. Over the tropical oceans, the semidiurnal pressure tides have an amplitude of $\sim$1 mb, which is comparable to the diurnal pressure tides over the United States where the pressure tides induce a diurnal amplitude of $\sim 10^{-6}$ s^{-1} in low-level convergence (Dai et al. 1999a). Therefore, the pressure tides over the tropical oceans are large enough to induce substantial diurnal variations in low-level convergence. Another possible (but likely small) contributor to the nighttime maximum is the relatively high water vapor saturation in maritime air at night (Fig. 7), as pointed out previously by Sui et al. (1997).

Over most of the oceanic areas, both the showery and nonshowery precipitation peaks from midnight to early morning (except DJF over the midlatitude North Pacific and North Atlantic where it peaks around noon to early afternoon), in contrast to land areas (Fig. 5). As pointed out by Dai (2001), nonshowery precipitation over the low-latitude oceans appears to be associated with showery precipitation (e.g., stratiform precipitation from anvil clouds follows moist convection). The similar phases of the diurnal cycles for maritime showery and nonshowery precipitation provide further evidence for such an association between the two types of precipitation over the low-latitude oceans.

For nondrizzle precipitation, which includes both showery and nonshowery precipitation and may be compared with rain gauge records, the phase pattern follows that of showery precipitation in summer (and in autumn and spring over low latitudes, not shown) and that of nonshowery precipitation in winter (and in autumn and spring over high latitudes, not shown) (Fig. 5). As shown by Fig. 6, the diurnal variation of showery precipitation dominates over that of nonshowery precipitation during summer over land areas, resulting in a large late-afternoon maximum in the nondrizzle precipitation frequency. During winter, showery and nonshowery precipitation are out of phase over land areas and cancel each other to a large extent, resulting in a weak nighttime maximum in nondrizzle precipitation over land areas (Fig. 6b).

Over the United States, the phase patterns (including

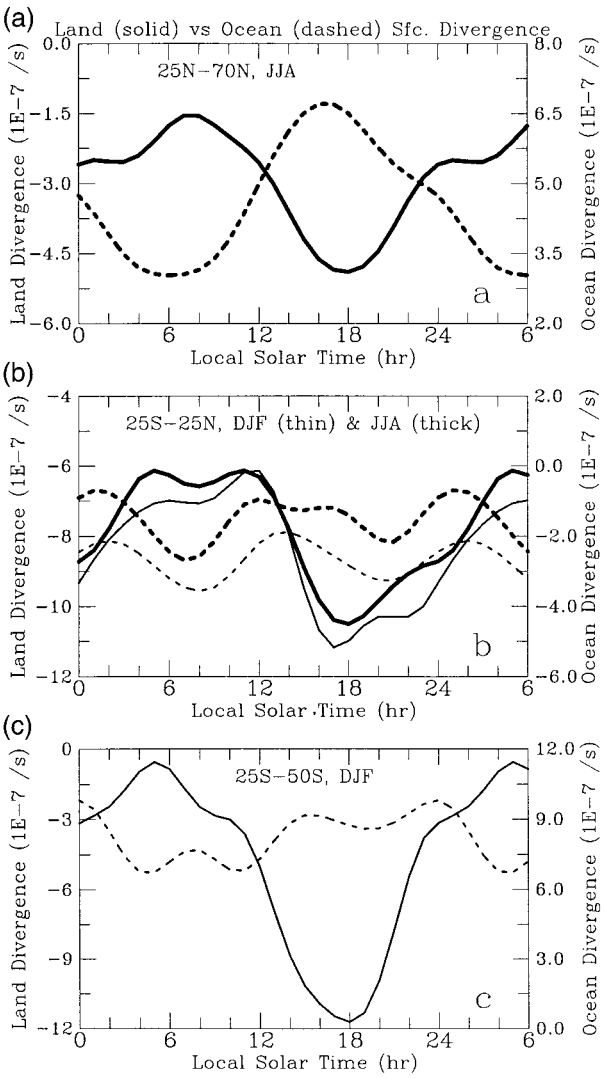

FIG. 9. Mean diurnal evolution of JJA (thick curves) and DJF (thin curves) surface wind divergence averaged (at each local solar time) over the land (solid curves) and oceanic (dashed curves) areas within 25°–75°N (a), 25°S–25°N (b), and 25°S–50°S (c). The wind divergence was derived from observed 3-hourly surface winds of the 1975–97 period (Dai and Deser 1999).

the midnight to early morning maximum over the central United States in summer) for nondrizzle precipitation frequency are very similar to those derived from hourly rain gauge records (e.g., Wallace 1975; Dai et al. 1999a). Furthermore, Fig. 5 shows that the morning (around 0600 LST) maximum in summer precipitation over the central United States results primarily from nonshowery precipitation that follows midnight showers and thunderstorms, which are propagated from the Rockies. The phase patterns for summer thunderstorms over the United States also match those based on hourly station data (Wallace 1975; Easterling and Robinson 1985). The morning maximum in the nondrizzle precipitation frequency over the midlatitude North Pacific and North Atlantic is in broad agreement with that of Kraus (1963), who analyzed about 10 yrs' (1952–61) data of 3-hourly weather reports from nine fixed weatherships in these regions. The morning maximum (around 0600 LST in JJA) over Japan is also consistent with the results of Oki and Musiake (1994), who analyzed hourly rain gauge data and found a morning (0500–0800 local standard time) maximum at most of the Japanese stations analyzed. Over the Amazon, the phases for showery, nonshowery, and nondrizzle precipitation are in broad agreement with those derived based on satellite rain-rate measurements (Lin et al. 2000).

c. The amplitude of the diurnal cycle

Figures 10 and 11 show the amplitude of the diurnal harmonic of DJF and JJA mean frequency of occurrence for drizzle, nondrizzle, showery and nonshowery precipitation, thunderstorms, and snow. In general, the patterns of the amplitude follow those of the mean frequencies (Dai 2001). The magnitude of the amplitude ranges from a few percent of the daily mean (insignificant) for winter nondrizzle and nonshowery precipitation and snow at high latitudes to over 50% of the mean (very significant) for summer showery precipitation and thunderstorms over land areas. The amplitude for the drizzle precipitation frequency is about 0.2%–0.5% over land areas and 1.0%–4.0% over the oceans, which are about 20%–30% of the daily mean values. For the nondrizzle precipitation frequency, the amplitude is about 1.5%–2.0% over most land areas, the North Pacific, and the Atlantic, and above 3.0% over tropical and southern Pacific and Indian Oceans. Seasonal variations in the amplitudes for drizzle and nondrizzle precipitation are small.

The amplitude for nonshowery precipitation is about 1.5%–2.0% in DJF and 1.0%–1.5% in JJA over most of the globe except over the arid areas such as northern Africa where it is about 0.2%–0.5%. The diurnal cycle of showery precipitation has a strong seasonal cycle over land areas with an amplitude of about 0.2%–0.5% in winter and 1.0%–3.0% in summer, whereas the seasonal cycle over the oceans is small with an amplitude of about 1.0%–3.0% in both DJF and JJA. The seasonal cycles of the amplitudes for showery and nonshowery precipitation are out of phase, which results in small seasonal variations in the diurnal cycle of nondrizzle precipitation.

d. The semidiurnal cycle, S_2

As shown by Figs. 1, 2, and 4, the semidiurnal cycle is considerably weaker than the diurnal cycle over most land areas and comparable to the diurnal cycle over the oceans. The amplitudes of the S_2 (not shown) are comparable to those of the S_1 (cf. Figs. 10 and 11) over the oceans. Over land areas, the amplitudes of the S_2 are generally less than half of those for the S_1. The phase

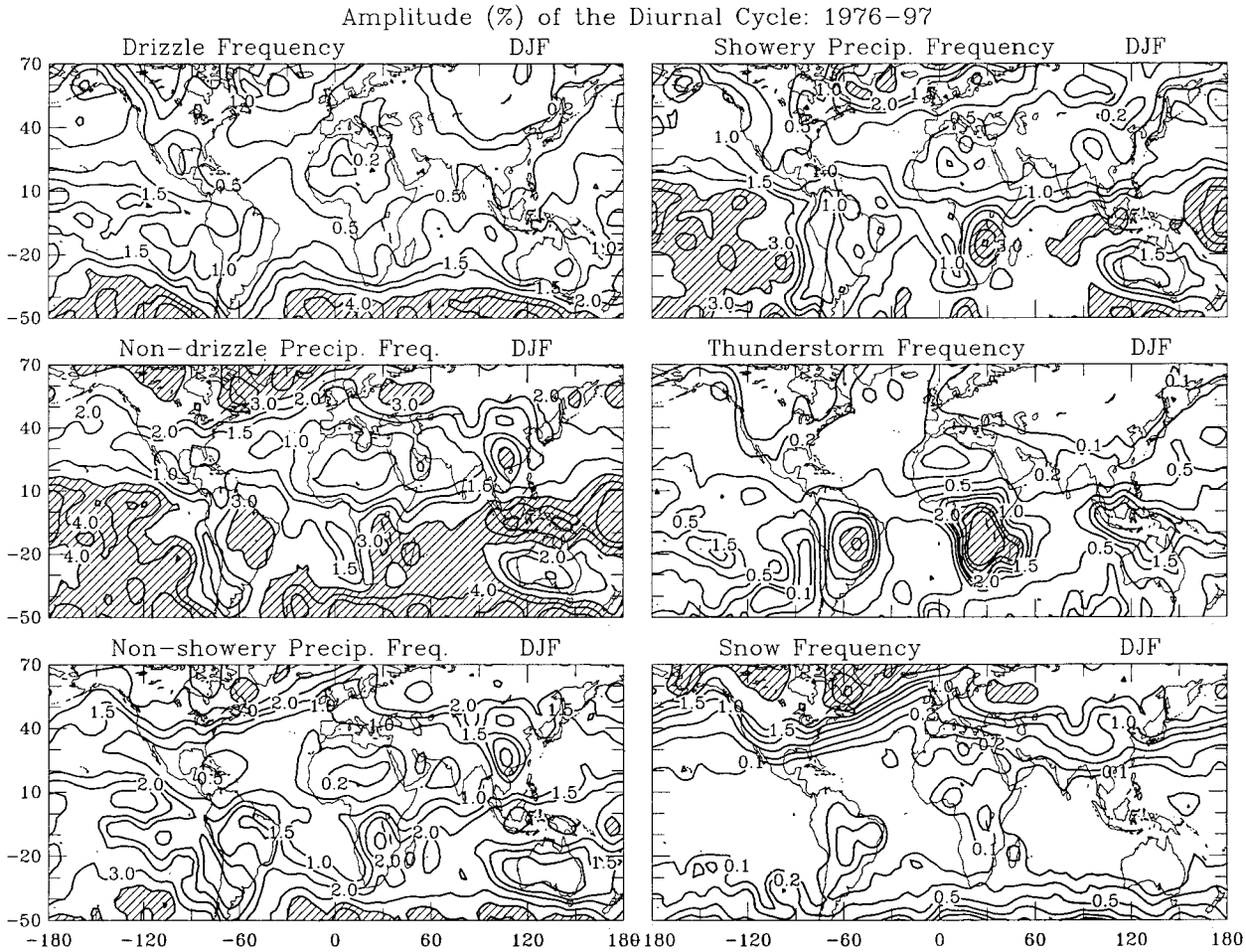

FIG. 10. Amplitude of the diurnal harmonic (S_1) of DJF mean frequency of occurrence (in percentage of time) for drizzle, nondrizzle, nonshowery and showery precipitation, thunderstorms, and snow. The amplitudes have been smoothed in space to reduce the small-scale noise. Contour intervals are 0.1%, 0.2%, 0.5%, 1.0%, 1.5%, 2.0%, 3.0%, 4.0%, and 5.0%. Values over 3.0% are hatched.

of the S_2 (not shown) is noisier than that of the S_1 (especially over the oceans where sampling errors for the S_2 are large), but in general the S_2 peaks around 0600–0800 and 1800–2000 LST over most land areas for drizzles, around 0900–1000 and 2100–2200 LST over northern mid- and high-latitude land areas for winter nonshowery and nondrizzle precipitation. Another coherent phase pattern of the S_2 is the early morning (0300–0400 LST) and afternoon (1500–1600 LST) peaks for summer nondrizzle and showery precipitation over most land areas, the western North Pacific, and many tropical and southern oceans. This appears to be consistent with the phase of semidiurnal pressure tides as mentioned above. Over the central North Pacific, the S_2 tends to peak around 0600–0800 and 1800–2000 LST in all types of precipitation, whereas it reaches maxima around 0400–0500 and 1600–1700 LST over the central North Atlantic. There are insufficient 3-hourly data over much of the equatorial Pacific and southern oceans for reliable estimates of the S_2 (6-hourly data and thus the S_1 have a better spatial coverage over these regions).

e. Zonal wave components

The diurnal and semidiurnal oscillations can be expanded into various zonal wave components at each latitude. Figure 12 shows the globally (from 50°S to 70°N, no data over many oceanic areas for the S_2) averaged amplitudes for the important wave components of the JJA diurnal and semidiurnal harmonics (similar plots for the other seasons). The wave modes with positive (negative) wavenumbers (s) travel toward the west (east), while the mode with $s = 0$ is a standing wave. In particular, the wave with $s = 1$ for the S_1 ($s = 2$ for the S_2) travels westward at the speed of the mean Sun. When expressed in the local time, this wave is independent of the longitude and is called the migrating tide in pressure and wind fields (Dai and Wang 1999; Dai and Deser 1999), whereas the other waves depend on both the local time and the longitude and are called nonmigrating tides (Haurwitz and Cowley 1973).

Figure 12 shows that both the diurnal and semidiurnal oscillations are dominated by the migrating waves

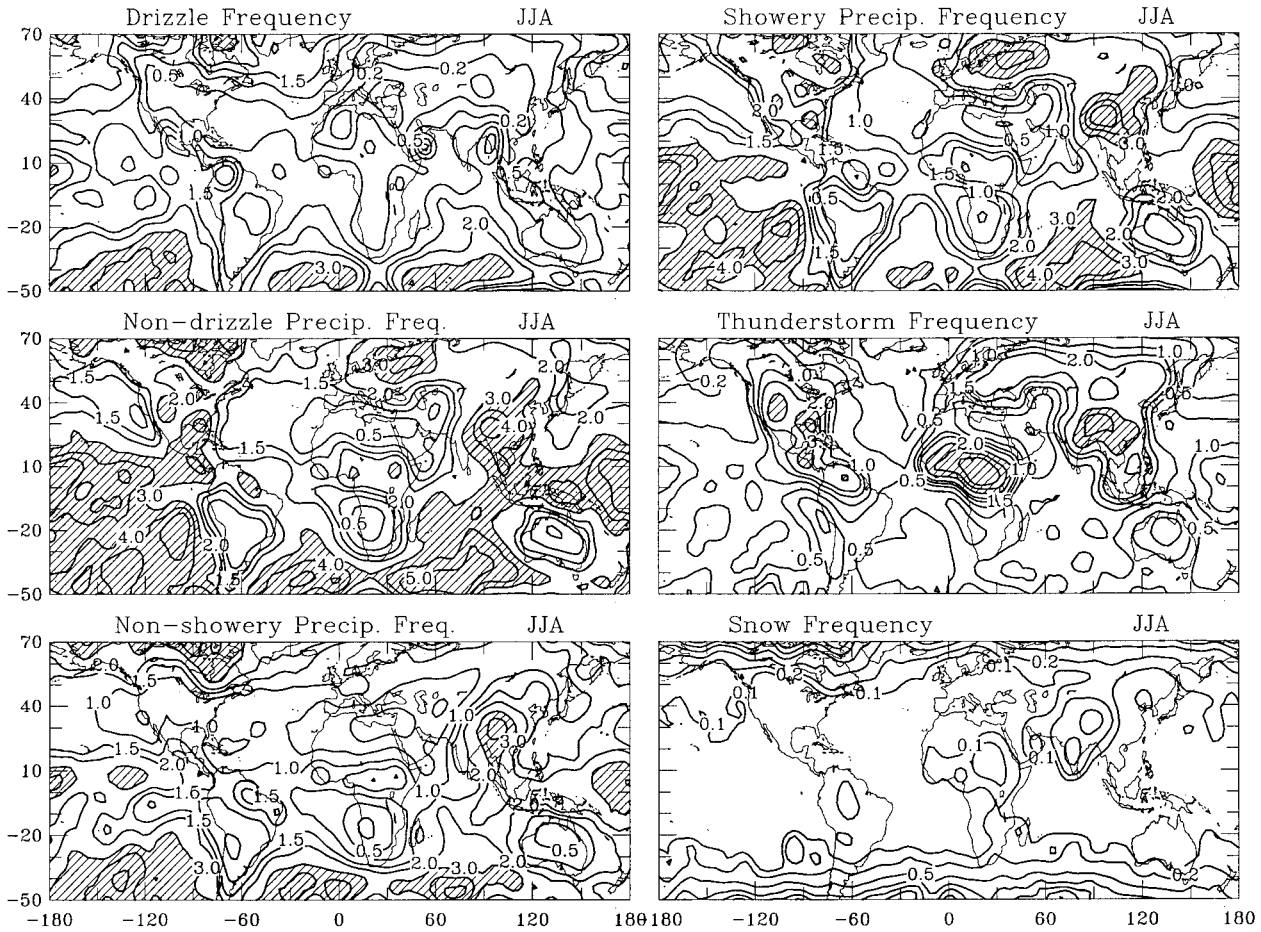

FIG. 11. Same as Fig. 10 but for JJA.

whose global mean amplitudes are about 3–4 times those of the nonmigrating waves. Contrary to surface pressure, whose global mean amplitude of the semidiurnal oscillation is greater than that of the diurnal oscillation (Haurwitz and Cowley 1973; Dai and Wang 1999), the global mean amplitudes of the diurnal oscillation of the precipitation and thunderstorm frequencies are larger than those of the semidiurnal oscillation, for both the migrating and nonmigrating components. This is consistent with the patterns shown in the anomaly data (Fig. 3) and agrees with the zonal wave components of surface winds and divergence (Dai and Deser 1999). These results suggest that while solar radiation is a major forcing for the diurnal variations in the precipitation and thunderstorm frequencies (as shown by the dominance of the migrating components in Fig. 12), the underlying physical processes for the diurnal variations in precipitation and thunderstorm frequencies are likely to be related to those for winds and divergence, but differ from those for pressure tides.

4. Summary

Mean diurnal variations in the frequency of occurrence for drizzle, nondrizzle, showery and nonshowery precipitation, thunderstorms, and snow over the globe (50°S–70°N) have been documented using 3-hourly weather reports (of precipitation and thunderstorm events) from about 15 000 GTS stations and the COADS for the 1975–97 period. Although there are sufficient data for resolving the diurnal and semidiurnal cycles in the precipitation and thunderstorm frequencies over most land areas, the North Pacific, and the North and tropical Atlantic, weather reports are sparse over the central and eastern tropical Pacific and southern oceans [especially for the semidiurnal cycle, see Fig. 2 of Dai (2001)], where our results have large sampling errors and should be interpreted with caution. The diurnal cycle of the nondrizzle precipitation frequency derived from the weather reports is consistent with that based on available rain gauge records over the United States, Japan, and other regions where data are available. The main results can be summarized as follows.

Except for winter mid- and high-latitudes, diurnal variations in the precipitation and thunderstorm frequencies are significant (especially over land areas and during summer), with diurnal amplitudes generally exceeding 20% of the daily mean values. The diurnal harmonic explains about 40%–80% of the total daily var-

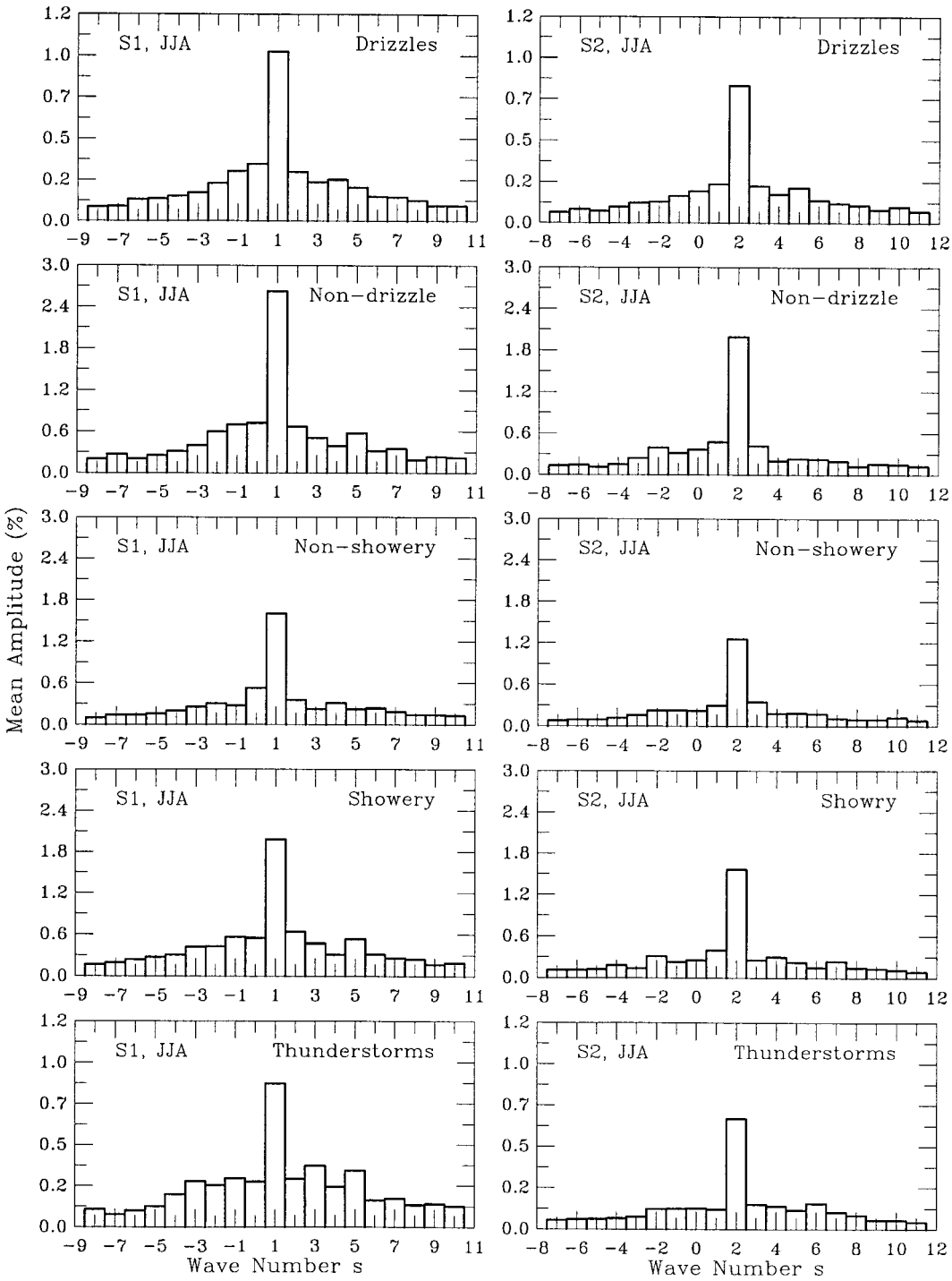

FIG. 12. Globally (50°S–70°N) averaged amplitudes of the (left) diurnal and (right) semidiurnal cycles at various zonal wave numbers for JJA mean frequency of occurrence for (top row) drizzle, (2d row) nondrizzle, (middle row) nonshowery and (4th row) showery precipitation, and (bottom row) thunderstorms. Plots for other seasons are similar.

iance over land areas, while it accounts for about 40% of the variance over the oceans. The semidiurnal harmonic accounts for about 15%–25% (20%–40%) of the daily variance over land (ocean) areas.

Drizzle and nonshowery precipitation generally occur most frequently in the morning around 0600 LST over most land areas and from midnight to 0400 LST over many oceanic areas. The diurnal amplitude of the drizzle frequency (in percentage of time) is about 0.2%–0.5% over land areas and 1.0%–4.0% over the oceans (which

are about 20%–30% of the daily mean values), whereas the amplitude for the nonshowery precipitation frequency is about 1.5%–2.0% in DJF and 1.0%–1.5% in JJA over most of the globe (≤20% of the mean).

The diurnal cycle of drizzle and nonshowery precipitation is approximately in phase with that of the relative humidity at the surface and in the lower troposphere, but out of phase with air temperature. It is suggested that the diurnal variations in atmospheric relative humidity contribute to the morning maxima (and afternoon minima) in the frequency of occurrence for drizzle and nonshowery precipitation, especially over land area.

Showery precipitation and thunderstorms occur much more frequently in the late afternoon than other times over most land areas in all seasons, with a diurnal amplitude exceeding 50% of the daily mean frequencies. Over the North Pacific, the North Atlantic, and many other oceanic areas adjacent to continents, showery precipitation occurs most frequently in the morning around 0600 LST, which is approximately out of phase with land areas. Over the tropical and southern oceans, showery precipitation tends to peak from midnight to 0400 LST. Thunderstorms tend to occur from midnight to early morning over most of the oceans.

The late-afternoon maximum for showery precipitation and thunderstorms over land areas is consistent with the late-afternoon maximum CAPE that results primarily from solar heating on the ground during the day. Over the oceans, diurnal variations of CAPE are small. However, the solar-driven diurnal cycle of moist convection over continents induces a large-scale diurnal circulation between the continents and the oceans, with maximum low-level convergence in the late afternoon (early morning) over the continents (oceans). It is suggested that the early morning maximum in maritime showery precipitation over the Northern Hemisphere and many tropical and southern oceans adjacent to continents results primarily from the land–ocean diurnal circulation. Larger low-level convergence induced by pressure tides and higher relative humidity at night than at other times may contribute to the nighttime maximum of maritime showery (and nonshowery) precipitation over remote oceans far away from continents.

Over most land areas, diurnal variations of showery precipitation predominate during summer, which results in a large late-afternoon maximum in nondrizzle precipitation frequency. During winter, showery and nonshowery precipitation are out of phase, resulting in a weak nighttime maximum in nondrizzle precipitation over most land areas. Over the central United States, summer showers and thunderstorms tend to peak around midnight whereas nonshowery precipitation occurs most frequently in the early morning around 0600 LST. Over the mid- and low-latitude oceans, showery and nonshowery precipitation both peak in the early morning. This further suggests that these two types of precipitation are physically related over the oceans (e.g., stratiform precipitation from anvil clouds follows deep convection).

The amplitudes of the semidiurnal cycle for the precipitation frequencies are comparable to those of the diurnal cycle over the oceans, but generally less than one-half of those for the diurnal cycle over land areas. In general, the semidiurnal cycle peaks around 0600–0800 and 1800–2000 LST over most land areas for drizzles, around 0900–1000 and 2100–2200 LST over northern mid- and high-latitude land areas for winter nonshowery and nondrizzle precipitation. The semidiurnal cycle for summer showery and nondrizzle precipitation peaks in the early morning (0300–0400 LST) and afternoon (1500–1600 LST) over most land areas, the western North Pacific, and many tropical and southern oceans. Over the central North Pacific, the semidiurnal cycle (for all types) tends to peak around 0600–0800 and 1800–2000 LST, whereas it peaks around 0400–0500 and 1600–1700 LST over the central North Atlantic.

The daily anomalies of the precipitation frequencies are dominated by the westward propagating waves (zonal wavenumber 1 for the diurnal cycle and zonal wavenumber 2 for the semidiurnal cycle). The global mean amplitude of the diurnal cycle exceeds that for the semidiurnal cycle, which agrees with those for surface winds and divergence but is in contrast to surface pressure tides.

More studies are needed to investigate the interactions between tidal variations in atmospheric pressure, winds, and divergence fields and the diurnal variations of precipitation, especially over the open oceans. The influence of landmasses on the diurnal cycle of maritime precipitation should also be investigated using global climate models.

Acknowledgments. I am grateful to Steve Worley, Dennis Joseph, and Gregg Walters for sharing their knowledge of surface observations. This study was supported by the ACACIA Consortium (CRIEPI, Japan; EPRI, California; KEMA Nederland B.V., the Netherlands; and the National Center for Atmospheric Research).

REFERENCES

Albright, M. D., 1985: Diurnal variation of deep convection and inferred precipitation in the central tropical Pacific during January–February 1979. *Mon. Wea. Rev.,* **113,** 1663–1680.

Augustine, J. A., 1984: The diurnal variation of large-scale inferred rainfall over the tropical Pacific Ocean during 1979. *Mon. Wea. Rev.,* **112,** 1745–1751.

Balling, R. C., Jr., 1985: Warm season nocturnal precipitation in the Great Plains of the United States. *J. Climate Appl. Meteor.,* **24,** 1383–1387.

Brier, G. W., and J. S. Simpson, 1969: Tropical cloudiness and precipitation related to pressure and tidal variations. *Quart. J. Roy. Meteor. Soc.,* **95,** 120–147.

Chang, A. T. C., L. S. Chiu, and G. Yang, 1995: Diurnal cycle of oceanic precipitation from SSM/I data. *Mon. Wea. Rev.,* **123,** 3371–3380.

Chen, S. S., and R. A. Houze, 1997: Diurnal variation and lifecycle of deep convective systems over the tropical Pacific warm pool. *Quart. J. Roy. Meteor. Soc.*, **123,** 357–388.

Dai, A., 2001: Global precipitation and thunderstorm frequencies. Part I: Seasonal and interannual variations. *J. Climate*, **14,** 1092–1111.

——, and C. Deser, 1999: Diurnal and semidiurnal variations in global surface wind and divergence fields. *J. Geophys. Res.*, **104,** 31 109–31 125.

——, and J. Wang, 1999: Diurnal and semidiurnal tides in global surface pressure fields. *J. Atmos. Sci.*, **56,** 3874–3891.

——, F. Giorgi, and K. E. Trenberth, 1999a: Observed and model simulated precipitation diurnal cycle over the contiguous United States. *J. Geophys. Res.*, **104,** 6377–6402.

——, K. E. Trenberth, and T. R. Karl, 1999b: Effects of clouds, soil moisture, precipitation and water vapor on diurnal temperature range. *J. Climate*, **12,** 2451–2473.

Easterling, D. R., and P. J. Robinson, 1985: The diurnal variations of thunderstorm activity in the United States. *J. Climate Appl. Meteor.*, **24,** 1048–1058.

Englehart, P. J., and A. V. Douglas, 1985: A statistical analysis of precipitation frequency in the conterminous United States, including comparisons with precipitation totals. *J. Climate Appl. Meteor.*, **24,** 350–362.

Foltz, G. S., and W. M. Gray, 1979: Diurnal variation in the troposphere's energy balance. *J. Atmos. Sci.*, **36,** 1450–1466.

Fu, R., A. D. DelGenio, and W. B. Rossow, 1990: Behavior of deep convective clouds in the tropical Pacific from ISCCP radiances. *J. Climate*, **3,** 1129–1152.

Garreaud, R. D., and J. M. Wallace, 1997: The diurnal march of convective cloudiness over the Americas. *Mon. Wea. Rev.*, **125,** 3157–3171.

Gray, W. M., and R. W. Jacobson Jr., 1977: Diurnal variation of deep cumulus convection. *Mon. Wea. Rev.*, **105,** 1171–1188.

Gruber, A., and T. S. Chen, 1988: Diurnal variation of outgoing longwave radiation. *J. Climatol.*, **8,** 1–16.

Hamilton, K., 1981a: Latent heat release as a possible forcing mechanism for atmospheric tides. *Mon. Wea. Rev.*, **109,** 3–17.

——, 1981b: A note on the observed diurnal and semidiurnal rainfall variations. *J. Geophys. Res.*, **86,** 12 122–12 126.

Hartmann, D. L., and E. E. Recker, 1986: Diurnal variation of outgoing longwave radiation in the tropics. *J. Climate Appl. Meteor.*, **25,** 800–812.

Haurwitz, B., and D. Cowley, 1973: The diurnal and semidiurnal barometric oscillations, global distribution, and annual variation. *Pure Appl. Geophys.*, **102,** 193–222.

Hendon, H. H., and K. Woodberry, 1993: The diurnal cycle of tropical convection. *J. Geophys. Res.*, **98,** 16 623–16 637.

Higgins, R. W., J. E. Janowiak, and Y.-P. Yao, 1996: A gridded hourly precipitation database for the United States (1963–1993). *NCEP/Climate Prediction Center ATLAS No. 1*, U.S. Dept. of Commerce, 47 pp.

Hu, C.-Y., and S.-S. Hong, 1989: Diurnal variations of precipitation frequencies in the Taiwan area. *Meteor. Bull.*, **35,** 65–88.

Janowiak, J. E., P. A. Arkin, and M. Morrissey, 1994: An examination of the diurnal cycle in oceanic tropical rainfall using satellite and in situ data. *Mon. Wea. Rev.*, **122,** 2296–2311.

Kalnay, E., and Coauthors, 1996: The NMC/NCAR 40-Year Reanalysis Project. *Bull. Amer. Meteor. Soc.*, **77,** 437–471.

Kraus, E. B., 1963: The diurnal precipitation change over the sea. *J. Atmos. Sci.*, **20,** 551–556.

Kousky, V., 1980: Diurnal rainfall variation in northeast Brazil. *Mon. Wea. Rev.*, **108,** 488–498.

Landin, M. G., and L. F. Bosart, 1989: The diurnal variation of precipitation in California and Nevada. *Mon. Wea. Rev.*, **117,** 1801–1816.

Lim, G.-H., and H.-J. Kwon, 1998: Diurnal variations of precipitation over South Korea and its implication. *J. Korean Meteor. Soc.*, **34,** 222–237.

Lin, X., L. D. Fowler, and D. A. Randall, 2000: Diurnal variability of the hydrologic cycle and radiative fluxes: Comparisons between observations and a GCM. *J. Climate*, **13,** 4159–4179.

Lindzen, R. S., 1978: Effect of daily variations of cumulonimbus activity on the atmospheric semidiurnal tide. *Mon. Wea. Rev.*, **106,** 526–533.

Majugu, A. W., 1986: Diagnostic study of the mean and seasonal diurnal variation of precipitation in East Africa. WMO Programme on Long-Range Forecasting, Res. Rep. Ser. No.6, 453 pp.

Malkus, J. S., 1964: Convective processes in the tropics. *Proc. Symp. on Tropical Meteorology*, Rotorua, New Zealand, 247–277.

McGary, M. M., and R. J. Reed, 1978: Diurnal variations in convective activity and precipitation during phases II and III of GATE. *Mon. Wea. Rev.*, **106,** 101–113.

Meisner, B., and P. Arkin, 1987: The relationship between large-scale convective rainfall and cold cloud over the Western Hemisphere during 1982–84. *Mon. Wea. Rev.*, **115,** 51–74.

Negri, A., R. Adler, E. Nelkin, and G. Huffman, 1994: Regional rainfall climatologies derived from Special Sensor Microwave Imager (SSM/I) data. *Bull. Amer. Meteor. Soc.*, **75,** 1165–1182.

Oki, T., and K. Musiake, 1994: Seasonal change of the diurnal cycle of precipitation over Japan and Malaysia. *J. Appl. Meteor.*, **33,** 1445–1463.

Randall, D. A., Harshvardhan, and D. A. Dazlich, 1991: Diurnal variability of the hydrologic cycle in a general circulation model. *J. Atmos. Sci.*, **48,** 40–62.

Reed, R. J., and K. D. Jaffe, 1981: Diurnal variation of summer convection over West Africa and the tropical eastern Atlantic during 1974 and 1978. *Mon. Wea. Rev.*, **109,** 2527–2534.

Riehl, H., and A. M. Miller, 1978: Differences between morning and evening temperatures of cloud tops over tropical continents and oceans. *Quart. J. Roy. Meteor. Soc.*, **104,** 757–764.

Riley, G. T., M. G. Landin, and L. F. Bosart, 1987: The diurnal variability of precipitation across the Central Rockies and adjacent Great Plains. *Mon. Wea. Rev.*, **115,** 1161–1172.

Sanders, F., and J. C. Freeman, 1983: Thunderstorms at sea. *Thunderstorm Morphology and Dynamics*, E. Kessler, Ed., Univ. of Oklahoma Press, 41–58.

Schwartz, B. E., and L. F. Bosart, 1979: The diurnal variability of Florida rainfall. *Mon. Wea. Rev.*, **107,** 1535–1545.

Sharma, A., A. Chang, and T. Wilheit, 1991: Estimation of the diurnal cycle of oceanic precipitation from SSM/I data. *Mon. Wea. Rev.*, **119,** 2168–2175.

Shin, K.-S., G. R. North, Y.-S. Ahn, and P. A. Arkin, 1990: Time scales and variability of area-averaged tropical oceanic rainfall. *Mon. Wea. Rev.*, **118,** 1507–1516.

Shinoda, M., T. Okatani, and M. Saloum, 1999: Diurnal variations of rainfall over Niger in the West Africa Sahel: A comparison between wet and drought years. *Int. J. Climatol.*, **19,** 81–94.

Short, D. A., and J. M. Wallace, 1980: Satellite-inferred morning-evening cloudiness changes. *Mon. Wea. Rev.*, **108,** 1160–1169.

Silva Dias, P. L., J. P. Bonatti, and V. E. Kousky, 1987: Diurnally forced tropical tropospheric circulation over South America. *Mon. Wea. Rev.*, **115,** 1465–1478.

Sui, C.-H., K.-M. Lau, Y. N. Takayabu, and D. A. Short, 1997: Diurnal variations in tropical oceanic cumulus convection during TOGA COARE. *J. Atmos. Sci.*, **54,** 639–655.

Tucker, D. F., 1993: Diurnal precipitation variations in south-central New Mexico. *Mon. Wea. Rev.*, **121,** 1979–1991.

Wallace, J. M., 1975: Diurnal variations in precipitation and thunderstorm frequency over the conterminous United States. *Mon. Wea. Rev.*, **103,** 406–419.

Woodruff, S. D., S. J. Lubker, K. Wolter, S. J. Worley, and J. D. Elms, 1993: Comprehensive ocean–atmosphere data set (COADS) release 1a: 1980–1992. *Earth Syst. Monit.*, **4,** 1–8.

Xu, K., and D. A. Randall, 1995: Impact of interactive radiative transfer on the macroscopic behavior of cumulus ensembles. Part II: Mechanisms for cloud-radiative interactions. *J. Atmos. Sci.*, **52,** 800–817.